A Near-Field-Based Gain and Pattern Measurement Technique for Probe-Fed Millimeter-Wave Antennas

Menglou Rao and Kamal Sarabandi

EDITOR'S NOTE

Xiu Yin Zhang

In this issue's "Measurements Corner" column, the authors present a fast, simple, and accurate near-field (NF)-to-far-field (FF) technique for gain and radiation pattern measurements of probe-fed millimeter-wave (mm-wave) antennas. The system uses a high-spatial-resolution nonintrusive probe to scan the NF in very close proximity to the antenna's surface, which significantly alleviates multipath effects and reduces the required scan area. In addition, for demonstration purposes, two mm-wave antennas are fabricated and tested by using the NF-to-FF technique. The result exhibits excellent accuracy. This research could thus facilitate probe-fed mm-wave antenna measurements for 5G communications.

Driven by the perpetual demand for higher data rates, extensive research efforts have been devoted to millimeter-wave (mm-wave) 5G technologies in recent years. Highly integrated mm-wave antennas for 5G user equipment are considered one of the key components in the realization of mm-wave-based mobile networks. An accurate characterization of antennas is as important as antenna design. Despite great advances in measurement capabilities over the years, we are still facing many difficulties in probe-based mm-wave antenna measurements. This article presents a fast, simple, and accurate near-field (NF)-to-far-field (FF) technique for gain and radiation pattern measurements of probe-fed mm-wave antennas. A setup based on an electro-optical (EO) NF measurement system (NeoScan) is utilized to measure the NF of the antenna under test (AUT). The system uses a high-spatial-resolution nonintrusive probe to scan the NF in very close proximity to the antenna's surface, which significantly alleviates multipath effects and reduces the required scan area. The radiation pattern of the AUT is computed using the NF-to-FF transformation. To obtain the gain of the AUT, a ground-backed dipole antenna is created and used as a gain standard. The absolute gain of the ground-backed dipole is characterized using the image method. Measurement accuracy is checked against the simulation. With the help of the standard gain antenna, the NF-to-FF method can be used to measure both the gain and radiation pattern of any type of probe-fed mm-wave antenna. For demonstration purposes, two test antennas, a horizontally polarized tapered slot antenna, and a dual-band vertically polarized hexagonal bridge antenna operating at 28 GHz are fabricated and characterized. Excellent agreement against full-wave simulation is achieved.

Digital Object Identifier 10.1109/MAP.2022.3210859
Date of current version: 6 December 2022

INTRODUCTION

The potential of large bandwidth and high data rates in the mm-wave region has made it an attractive candidate for many wireless applications. The transition from the current 4G mobile network to 5G further drives R&D efforts in mm-wave frequencies. Consequently, there is great research interest in mm-wave antennas that can be fully integrated with radio-frequency (RF) circuits on the same chip.

An accurate characterization of antennas is of great importance in system design. The key parameters include antenna impedance matching, gain, and radiation pattern. Conventionally, antennas are connected to test equipment using standard coaxial cables or

 1045-9243/22©2022IEEE

waveguides. However, introducing such transitions imposes severe limitations on antenna measurements in the mm-wave frequency region because their sizes are comparable with or even larger than the AUT. The uncertainty introduced by the interaction between the transition fixtures and the antenna is difficult to predict. It has been experimentally demonstrated that connectors can strongly disturb the antenna's radiation pattern and cause serious measurement errors [1]. Additionally, antennas are more frequently integrated onto semiconductor chips. The measurements using transition fixtures do not fully present the actual performance of the antenna. For these reasons, it is preferred to feed the AUT with an RF probe during measurements, which makes it possible to characterize the AUT at the point where the RF component will be connected in the final application.

The matching performance of an antenna can be directly evaluated from the reflection coefficient measurement using a network analyzer, whereas the gain and radiation pattern measurements are more complicated. The first gain measurement of an on-wafer antenna is reported in [2], where a pair of identical antennas are placed at a distance R, and the gain is extracted from the S_{21} measurement. As the positions of the antennas are fixed, only the gain in the maximum radiation direction is measured. An improved setup that allows for antenna radiation pattern measurements is presented in [3]. An open-ended waveguide is attached to a customized Plexiglas fixture and used as a sampling antenna. The fixture arm is rotated by a stepper motor along a virtual arc extending from −90 to 90°, thus the pattern in the upper half plane can be measured. Similar FF pattern measurements of on-chip antennas are reported in [4] and [5]. The first 3D radiation pattern measurement setup is proposed in [1]. With two rotating arms, the sampling antenna can move on the surface of a sphere around the AUT, except the region blocked by the probe positioner. All of the aforementioned gain and radiation pattern measurements are conducted in the FF region of both the test and sampling antennas. They involve an expensive customized probe station design and complex mechanical structures. Moreover, at mm-wave frequencies, reflections and scattering from the measurement setup, the twist of cables, and misalignment of the sampling antenna can cause significant phase errors. As a consequence, inconsistent gain, distorted radiation patterns, and intense ripples are always reported in the literature [1], [2], [3], [4], [5].

NF-to-FF methods can alleviate these issues and can be implemented in a much more compact range. However, performing such techniques on probe-fed mm-wave antennas is extremely challenging. Conventional NF measurement systems use small metallic antennas such as a short dipole [6] or an open-ended waveguide [7] as the NF sampling probe. The AUT needs to be placed in the FF region of the probe so that the probe does not perturb the measured NF. For a short dipole, the FF criterion can be obtained by requiring the radiating component to be much larger than the Biot–Savart's component, i.e.,

$$\frac{1}{kR} \ll 1 \tag{1}$$

where R is the distance between the source and the observation point, and k is the wavenumber in free space. If we set a factor of 10 for the ratio of the radiating component to the nonradiating component, the FF distance is

$$R = \frac{10}{k} = 1.6\,\lambda. \tag{2}$$

With this constraint, it is very difficult to accurately measure the NF of an mm-wave antenna on a probe station because the magnitude of the multiple scattering from the probe station and the probe itself is comparable to the direct signal from the AUT. In addition, based on the sampling distance, a certain scan area is required to ensure accuracy of the FF pattern over a specified angular range. Nevertheless, the scan range on a probe station is very limited. As a result, the FF pattern is only valid over a very small angular range or even completely wrong [6].

To circumvent issues with conventional metallic probes, EO probes have been exploited as an alternative solution. The successful implementation of EO systems that characterize antennas and arrays has been reported previously [8], [9], [10], [11], [12]. In [8], EO crystals are used to measure the NF patterns of a 4-GHz patch antenna. The amplitude and phase maps of three orthogonal electric-field components are presented. A continuous-wave EO NF mapping system is developed to characterize a dual-band (2.1 and 4.8 GHz) circularly polarized phased array [9] and an X band active electronically scanned array [10]. In [11], a commercial EO NF scan system is employed to obtain the FF radiation pattern of a miniaturized very high-frequency antenna. In [12], an EO sensor is utilized to map the NF of a 20-GHz pyramidal horn antenna. The FF radiation pattern is then computed using the NF-to-FF transformation. However, none of the aforementioned measurements are performed in the mm-wave frequency region (most of them are performed at frequencies below 10 GHz), and the antennas are tested in cluster-free environments. It is not clear whether the EO NF measurement is as effective at mm-wave frequencies, especially on a probe station where the reflection and scattering from the probe station and surrounding environment can be very strong. Furthermore, [8], [9], [10], and [12] only provide the radiation patterns of the AUTs. In [11], a standard transverse electromagnetic (TEM) cell is used to calibrate the EO probe so that the absolute gain of the AUT can be determined based on the NF data. Unfortunately, TEM cells are not available at mm-wave frequencies. Another way to obtain the gain of the AUT based on an NF setup is to use the NF gain comparison technique [13]. In this approach, the gain of the AUT is determined by establishing a comparison between the measured NF of the AUT and that of a standard antenna with a known gain. In [7], a pyramidal horn antenna is used as the reference. However, as the horn antenna has a different feeding structure, it is not feasible to replace the AUT with the horn antenna while maintaining all measurement parameters unchanged. A more practical

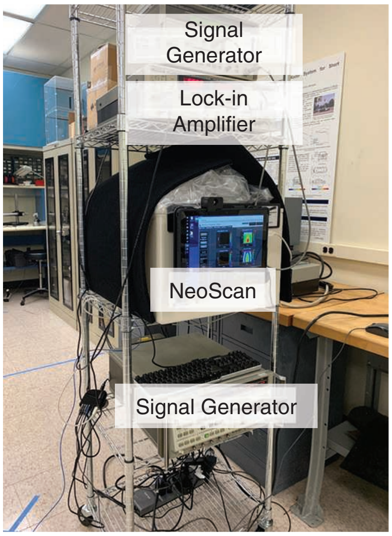

FIGURE 1. The NeoScan NF mapping system.

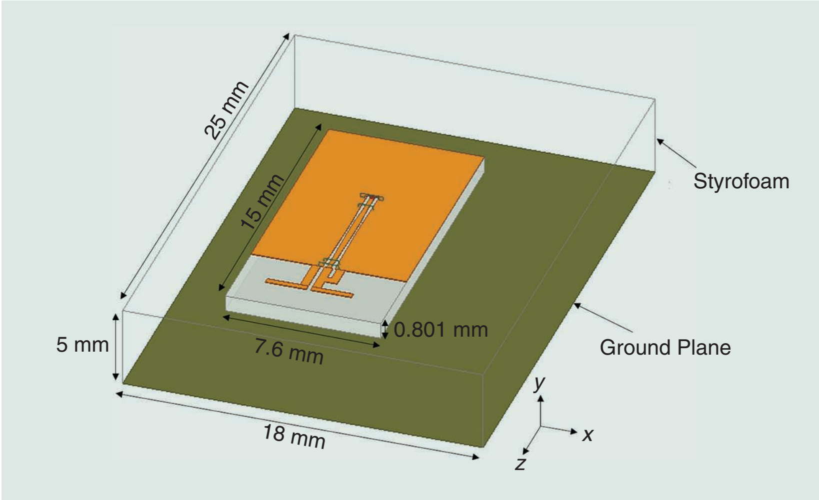

FIGURE 2. The ground-backed dipole antenna.

and accurate way is to have a probe-fed standard gain antenna. Unfortunately, such an antenna does not currently exist.

This article directly addresses the aforementioned issues and presents a simple and inexpensive NF-to-FF technique that can simultaneously obtain the gain and radiation pattern of a probe-fed mm-wave antenna. A commercial NF scan system (NeoScan [14], developed by EMAG Technologies) is used to map the NF of the antenna. The system utilizes an extremely small nonmetallic EO probe that has the capability to accurately sample the electric fields in close proximity to the antenna's surface (<1 mm) with very high spatial resolution (minimum sampling interval $<10\ \mu$m). Thanks to the small sampling distance, multipath effects become negligible compared with the direct signal, and the required scan area is reduced substantially. To directly characterize the gain of the AUT on the same setup, we created a probe-fed, ground-backed dipole antenna, implemented the image method to accurately characterize its gain, and then used it as the gain standard. With the standard gain antenna, the NF-to-FF method can provide both the gain and radiation pattern of any type of probe-fed mm-wave antennas. This measurement technique eliminates the need for numerous custom-built test fixtures and complicated measurement setups and provides very accurate results. Furthermore, this method is especially useful for the characterization of radiation performance (i.e., gain, radiation pattern, and scan performance) of compact mm-wave phased arrays for 5G applications. In these applications, the antenna elements are closely spaced and fed with various phase excitations to realize beam steering. Directly measuring the array patterns by exciting all the elements with the desired phase is a cumbersome task. In [15], [16], and [17], the FF radiation patterns and scan patterns of the arrays are recreated by superimposing the individually measured FFs of each element. As the superposition is performed on the phasors of the FFs of each element, accurate phase measurement is required to produce the correct array pattern. As mentioned earlier, significant phase errors commonly occur in FF measurements. In [15], [16], and [17], different degrees of pattern distortion are observed. On the other hand, in the proposed NF-to-FF method, the superposition is performed on the calibrated complex NF data of each element, which can be precisely measured using the very NF scan system. In our recent work [18], it is demonstrated that the proposed method is able to characterize the radiation performance of a 1×4 phased array with high-level accuracy.

The article is organized as follows: the theories of both the image and NF-to-FF methods are introduced in the "Image Method for Gain Measurement" and "NF-to-FF Gain and Pattern Measurements" sections, respectively. The "Standard-Gain Ground-Backed Dipole Antenna" section provides the design details of a ground-back dipole and demonstrates how the image method is implemented to obtain the absolute gain of the antenna. In the " Examples of Using the NF-to-FF Method" section, gain and radiation pattern measurements using the NF-to-FF technique are demonstrated through two examples: a horizontally polarized tapered slot antenna and a vertically polarized hexagonal antenna are used as test antennas, and the ground-backed dipole antenna is used as the gain standard. The NFs of all three antennas are measured, and the radiation patterns are evaluated using the NF-to-FF transformation. The relative gains of the AUTs are then compared with the known gain

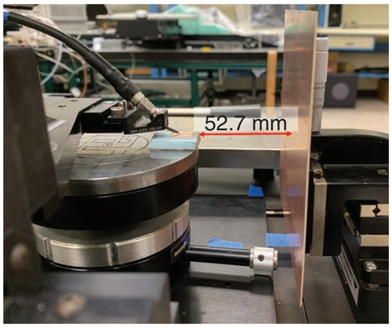

FIGURE 3. The setup for the absolute gain measurement using the image method.

of the standard antenna to obtain the absolute values.

THE IMAGE METHOD FOR GAIN MEASUREMENT

The image method proposed by Purcell [19] is an alternative approach to the standard two-antenna method, where two identical antennas are required to determine the antenna gain. In the method, instead of employing a twin antenna, a flat perfect conductor is used to generate an image of the AUT. The distance between the reflector and the AUT is $r/2$, and r must satisfy the FF criterion

$$r > \frac{2D^2}{\lambda} \tag{3}$$

where D is the maximum dimension of the antenna, and λ is the free-space wavelength at the operating frequency. Based on the Friis transmission formula, the gain of the antenna along the boresight direction can be calculated from

$$G(\mathrm{dB}) = 10\log_{10}\left(\frac{4\pi r}{\lambda}\right) + 5\log_{10}\left(\frac{P_r}{P_t}\right) \tag{4}$$

where P_t is the transmitted power, and P_r is the received power. The ratio P_r/P_t is given by

$$\frac{P_r}{P_t} = |S'_{11} - S_{11}|^2 \tag{5}$$

where S'_{11} and S_{11} are the reflection coefficients of the AUT with and without the reflector, respectively.

The feasibility of this method at mm-wave frequencies was demonstrated in [20], [21], and [22]. In [22], the impact of the size and alignment of the reflecting plate is thoroughly studied. As a rule of thumb, the size of the reflector must be much larger than the wavelength and the 3-dB footprint of the antenna on the reflector to produce accurate results.

The image method is a very efficient way to measure the absolute gain of a linearly polarized probe-fed antenna because it obviates the need for multiple antennas. This method is mostly suitable for antennas with a small electrical aperture and relatively short FF distance. For antennas with a large electrical aperture and narrow beamwidth, the size of the reflector becomes impractically large, and even a slight misalignment can cause significant errors. Furthermore, if the antenna radiates elliptically polarized waves, (4) needs to be modified to account for the polarization mismatch between the reflected waves and the antenna [23]. This method fails for circularly polarized antennas as the polarization of the reflected wave is perpendicular to that of the antenna.

In this article, the image method is used as an auxiliary step to provide an accurate gain measurement of a probe-fed, ground-backed dipole antenna, which is then used as the gain standard

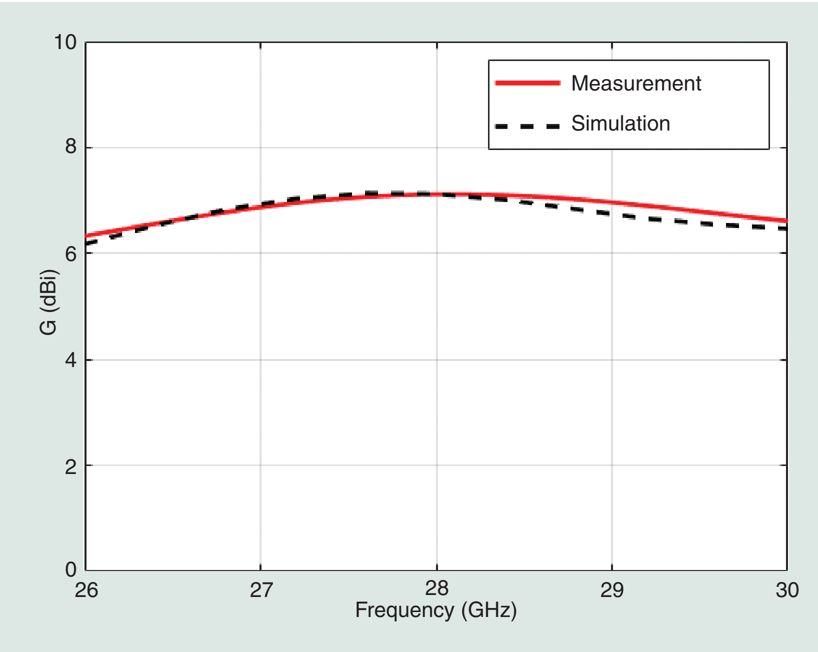

FIGURE 4. Measured and simulated absolute gains of the dipole antenna from 26 to 30 GHz.

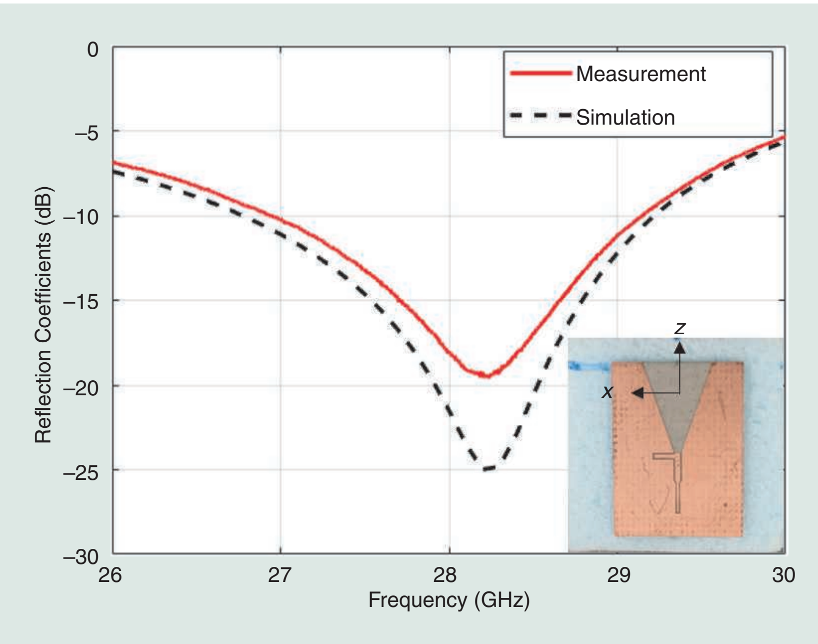

FIGURE 5. Geometry and reflection coefficients of the tapered slot antenna.

in the NF-to-FF method. A detailed design and measurement procedure will be presented in the "Standard-Gain Ground-Backed Dipole Antenna" section. Variations of the image method implemented on different types of antennas are outside the scope of the article and will not be discussed further.

NF-TO-FF GAIN AND PATTERN MEASUREMENTS

A more versatile way of measuring the gain of an antenna is the gain comparison method. Unlike the conventional gain comparison method, which is usually performed in the FF region, the NF gain comparison method is completely based on NF measurements. Therefore, it can be implemented in a much more compact range and avoid issues commonly associated with FF measurements. The technique requires a probe-fed standard gain antenna. Initially, NF measurements are performed, and the FF patterns are computed using the NF-to-FF transformation. Then the relative gains are compared with the known gain of the standard antenna to yield the absolute values. The method needs two sets of measurements. In one set, the NF measurement is performed on the standard antenna, and the radiation pattern (uncalibrated) is evaluated based on the NF data. In the other set, the standard antenna is replaced with the AUT, and the same procedure is repeated to obtain the radiation pattern of the AUT. Based on the uncalibrated radiation patterns, the relative gain of the AUT to the standard antenna ΔG can be obtained. Knowing the actual gain of the standard antenna G_{std}, we can derive the absolute gain of the AUT from

$$G_{\text{AUT}}(\text{dB}) = G_{\text{std}}(\text{dB}) + \Delta G(\text{dB}) \quad (6)$$

where ΔG is the difference between the values in the direction where the absolute gain of the standard antenna is evaluated. It should be noted that the system's setup, geometrical arrangement, placement of cables, and input power in both sets need to be maintained the same way. This requirement is very difficult to satisfy if a standard pyramidal horn antenna is used as the reference as a horn antenna has a different feeding structure and it is hard to place it properly on a chuck.

The use of the EO probe is key to the success of the NF-to-FF method. Traditional NF measurements use either a short dipole or an open-ended waveguide as the sampling probe, which is typically placed far away from the AUT to avoid disturbing the fields. As a consequence, measurements usually suffer from multipath effects from the probe station and do not provide satisfactory results. In contrast, EO probes can sample the electric field in close proximity to the antenna's surface with very high spatial resolution due to their noninvasive nature and small size, which substantially eliminates multipath effects and reduces the scan area. In this article, we use a commercial EO NF scan system called *NeoScan*. The EO field probe features an extremely small size and is all dielectric, which guarantees RF noninvasiveness of the probe. According to the data sheet, the probe can be placed as close as $\lambda/50$ (λ is the free-space wavelength at the operating frequency) to the antenna's surface without disturbing the

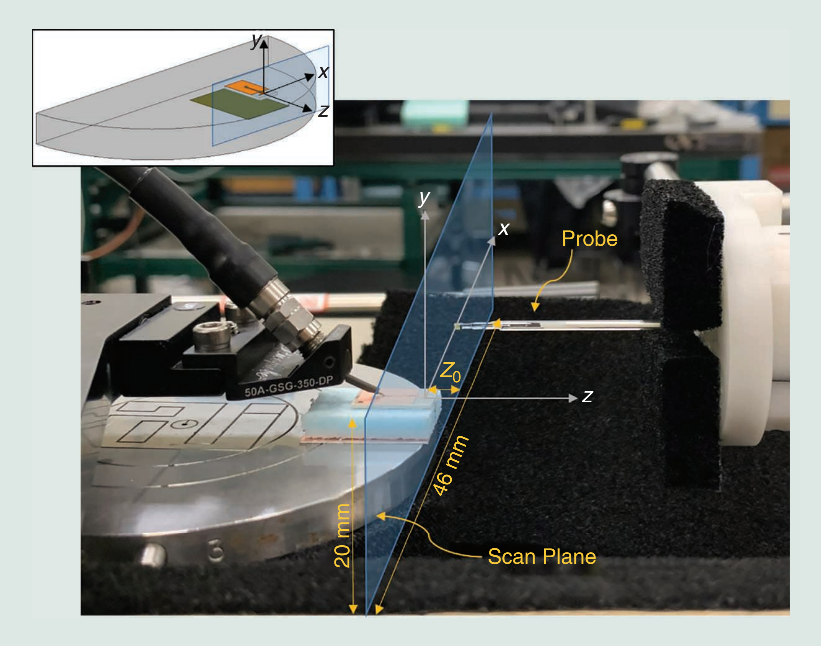

FIGURE 6. The NF scanning configuration.

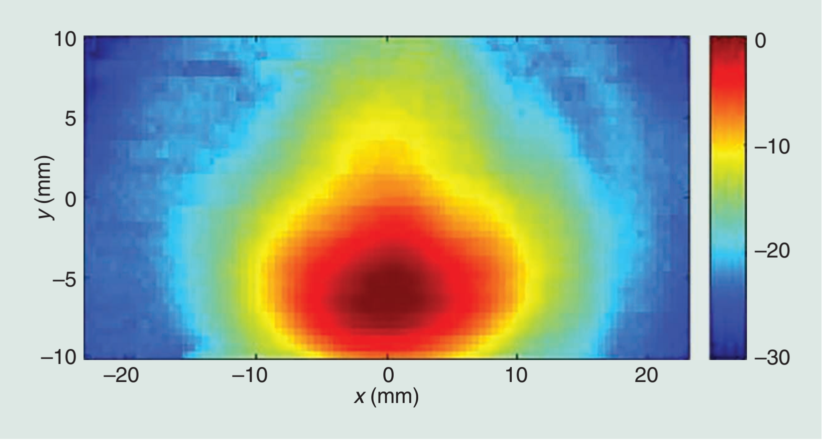

FIGURE 7. The NF distribution of the planar dipole antenna (unit: decibels).

measured field. In our measurements, the distance is chosen to be 1 mm, corresponding to 0.1 λ at 28 GHz. The system setup is shown in Figure 1.

The NF-to-FF method can be used to measure antennas with arbitrary patterns and polarizations. The limiting factor here is the probe station. A typical probe station has a metallic chuck and a built-in microscope, which can affect antenna performance. For this type of probe station, only antennas having boresight radiation patterns can be characterized accurately. To measure antennas that have upwards and/or downward radiation, necessary modifications to the measurement setup are needed, including replacing the metallic chuck with a wafer chuck, or using a dielectric foam holder, and replacing the fixed microscope with a moveable one [24].

The accuracy of the measurement is closely related to the precision of the phase center. For antennas without a well-defined phase center, this method may not predict accurate results.

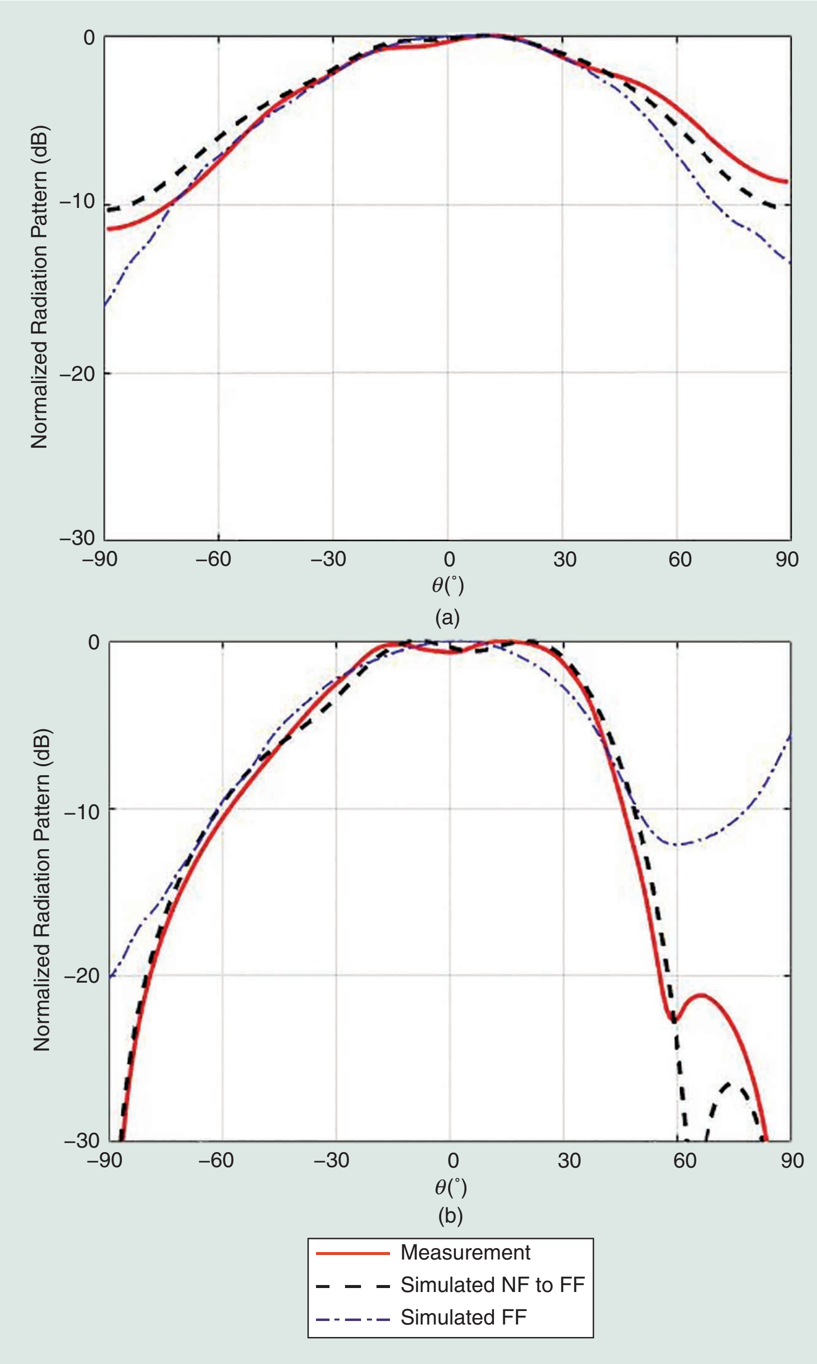

FIGURE 8. Normalized radiation patterns of the planar dipole in the (a) *xz*-plane and (b) *yz*- plane.

A STANDARD-GAIN GROUND-BACKED DIPOLE ANTENNA

As mentioned in the “NF-to-FF Gain and Pattern Measurements” section, the NF-to-FF method needs a standard gain antenna to obtain the gain of the AUT. Unfortunately, there are no probe-fed standard gain antennas currently available on the market. Half-wavelength dipoles are universally accepted as gain standards due to their high degree of polarization purity. Here we design a 28-GHz ground-backed planar dipole antenna as the gain standard. The geometry of the antenna, along with its dimensions, is illustrated in Figure 2. The dipole is fabricated on a Rogers 4003C laminate ($\epsilon_r = 3.55$, $\tan\delta = 0.0027$) with a thickness of 0.801 mm and is placed 5-mm above the ground plane. Styrofoam is used to support the antenna above the ground plane. The reason for adding a ground plane to the dipole is that the performance of the standard gain antenna needs to be stable to ensure accuracy of the gain comparison method. Without the ground plane, performance would be affected by the chuck, which would compromise accuracy of the NF-to-FF gain measurement. A balun is implemented for the transition from the standard ground-signal-ground (GSG) probe terminal to the balanced coplanar stripline. It should be noted that the balun is considered an integral part of the antenna. Proper de-embedding techniques are needed if differential input impedance of the antenna is desired [25].

The image method is used to calibrate the gain of the ground-backed dipole antenna. Figure 3 shows the arrangement of the antenna on the probe station for the measurement. The antenna is placed at the edge of the chuck and fed by a GSG RF probe (Picoprobe 50 A-GSG-350-DP). A network analyzer (Agilent 8722ES) is connected to the RF probe to measure reflection coefficients of the antenna. The system is calibrated to the probe tips using a standard calibration substrate (GGB Industries Inc. model CS-9). A large, flat conductor is placed in front of the antenna. The dimensions of the reflector are 12 cm × 12 cm. The distance between the phase center of the antenna and the reflector is 52.7 mm. We first measure the reflection coefficients of the AUT with the reflector (S'_{11}) then remove the reflector and take the measurement again (S_{11}). To reduce the effects of multiple reflection and edge diffraction, proper gating is applied to the time-domain response [26]. The absolute gain in the $+\hat{z}$ direction from 26 to 30 GHz is obtained using (4) and (5) and plotted in Figure 4. The measurement is in excellent agreement with the simulation. The absolute gain of the ground-backed dipole antenna is 7.123 dBi at 28 GHz.

EXAMPLES OF USING THE NF-TO-FF METHOD

For demonstration purposes, two 28-GHz antennas are fabricated and then tested using the NF-to-FF method. The first antenna is a horizontally polarized tapered slot antenna [27], and the second one is a vertically polarized hexagonal bridge antenna [18].

A HORIZONTALLY POLARIZED TAPERED SLOT ANTENNA

The tapered slot antenna is fabricated on a Rogers 4003 C substrate with a thickness of 0.801 mm. The geometry of the antenna, together with the simulated and measured refection coefficients, are shown in Figure 5.

We first measure the NF distribution of the standard gain dipole antenna and then compute its radiation pattern. For the planar-scanning configuration illustrated in Figure 6, the probe moves on a rectangular grid at a fixed distance $z_0 = 1$ mm from the center of the antenna. The scan area is 46 mm × 20 mm, and the sampling resolution is set to 0.5 mm. In the FF region, the electric field can be expressed as [28]

$$\mathbf{E}(\mathbf{r}) = jk_0 \frac{e^{-jk_0 r}}{2\pi r} \times [\hat{\boldsymbol{\theta}}(A_x \cos\phi + A_y \sin\phi) + \hat{\boldsymbol{\phi}} \cos\theta (A_y \cos\phi - A_x \sin\phi)] \tag{7}$$

where θ and ϕ denote the direction of observation. A_x and A_y are tangential components of the vector amplitude in the scanned plane and are related to the measured electric field by

$$\mathbf{A}_t(k_x, k_y) = e^{jk_z z_0} \iint_{-\infty}^{+\infty} \mathbf{E}_t(x, y, z_0) e^{jk_x x + jk_y y} dxdy \tag{8}$$

In the observation direction (θ, ϕ),

$$k_x = k_0 \sin\theta \cos\phi$$
$$k_y = K_0 \sin\theta \sin\phi$$
$$k_z = \sqrt{k_0^2 - k_x^2 - k_y^2}. \tag{9}$$

The measured NF distribution of the planar dipole is mapped in Figure 7. The asymmetry in the y-direction is due to the ground plane underneath the antenna. The small asymmetry in the x-direction is due to the presence of the balun on one side of the antenna, which perturbs the symmetry. The normalized radiation patterns in the xz- and yz-planes are plotted in Figure 8(a) and (b), respectively. For comparison, the simulated FF radiation patterns are also plotted in the figure. The measured patterns diverge from the simulation at large angles because of the finite size of the scan area. To better evaluate the measured results, we extract the NF distribution from the simulation and use it to compute the FF patterns. As displayed in Figure 8, the measured radiation patterns agree well with the simulated NF-to-FF patterns. The drop in the gain value at approximately $\theta = -5°$ in the yz-plane is due to abrupt truncation of the scan plane. Then the NF measurement is performed on the tapered slot antenna, and the radiation pattern in the xz-plane is computed and calibrated to obtain the absolute gain using (6). It should be pointed out that the entire process only requires lifting/landing the RF probe and replacing the standard dipole antenna with the tapered slot antenna (the AUT); all other measurement parameters for the two sets of measurements are maintained exactly the same way. Figure 9 shows the NF distribution of the tapered slot antenna. The asymmetry in the x-direction is due to the open stub, while the asymmetry in the y-direction is because of the metallic chuck under the antenna. Figure 10(a) and (b) shows the normalized radiation patterns of the tapered slot antenna in the xz- and yz-planes, respectively. Due to the metallic chuck, the maximum radiation shifts upward by roughly 10° in the yz-plane. If we include the chuck in the simulation, the measured radiation pattern agrees well with the simulation. The uncalibrated radiation pattern of the tapered slot antenna in the xz-plane is then compared with that

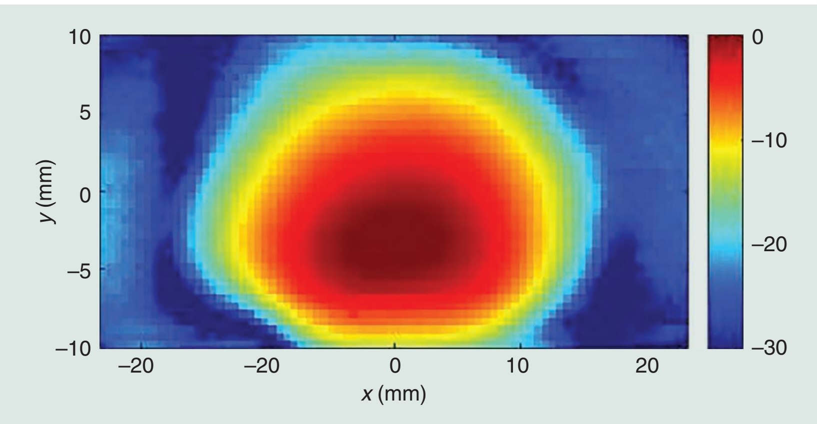

FIGURE 9. The NF distribution of the tapered slot antenna (unit: decibels).

of the standard antenna, as presented in Figure 11. The value at $\theta = 0°$ for the tapered slot antenna is 1.377-dB higher than that for the standard gain antenna. As the absolute gain of the standard gain antenna is 7.123 dBi, the absolute gain of the tapered slot antenna in the $+\hat{z}$ direction is 8.5 dBi.

For comparison, we also measured the gain of the tapered slot antenna using the image method. The results are listed in Table 1, along with the simulated gain. The measured gains agree well with the simulation.

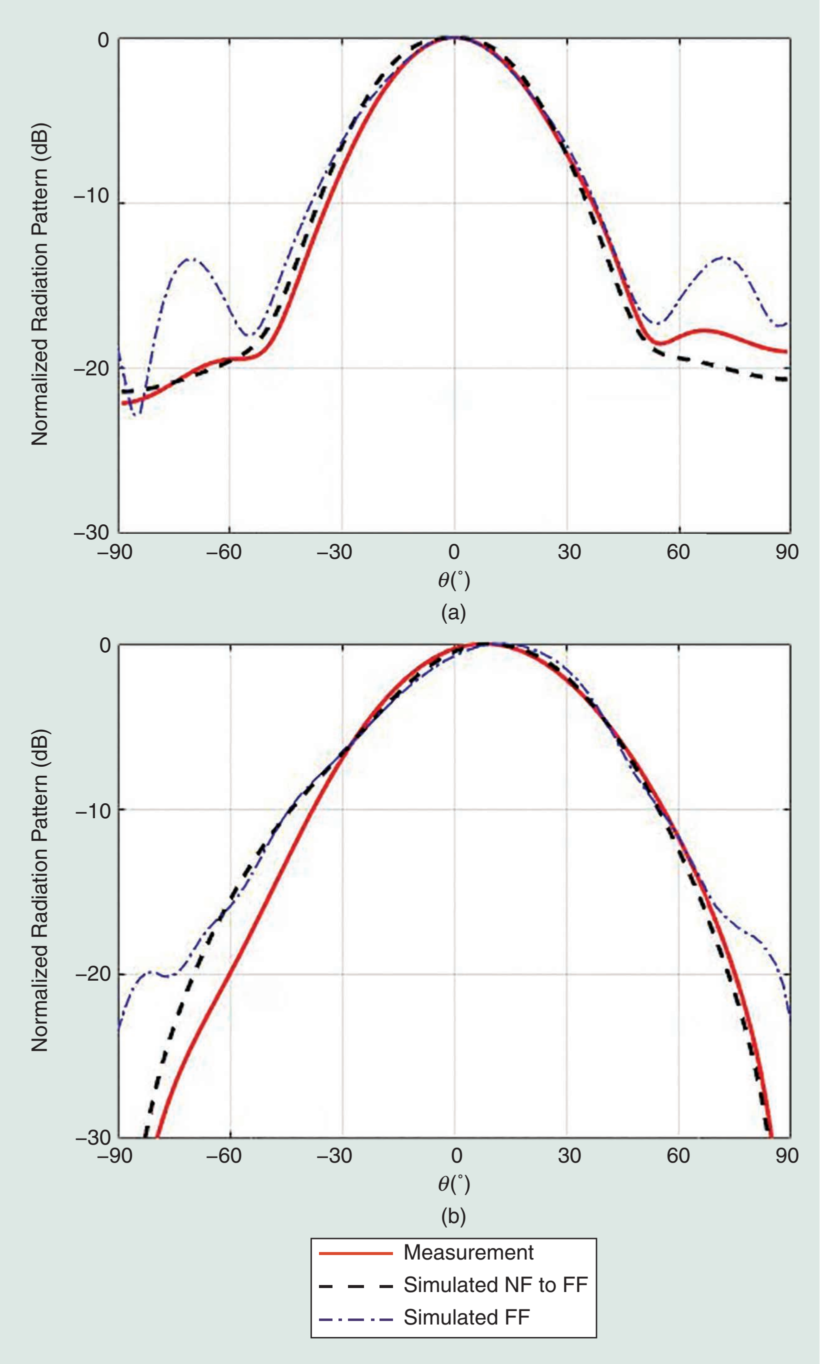

FIGURE 10. Normalized radiation patterns of the tapered slot antenna in the (a) *xz*-plane and (b) *yz*- plane.

A VERTICALLY POLARIZED HEXAGONAL BRIDGE ANTENNA

The second example is the vertically polarized hexagonal bridge antenna reported in [18]. The antenna is fabricated on a multilayer RO4003C substrate with a total height of 1.12 mm. The antenna geometry and measured reflection coefficients are adapted from the original article and presented in Figure 12 for the reader's convenience. In [18], the NF measurements are used only to determine the normalized radiation patterns of the antenna. The image method is used to obtain the absolute gain. Here we use the NF comparison method to characterize the gain of the antenna and compare the result with the value reported in [18].

Following the same procedure, we measured the NF distribution of both the standard gain dipole and hexagonal bridge antennas. The uncalibrated radiation patterns of the standard gain dipole and the hexagonal bridge antenna in the *xz*-plane are plotted in Figure 13. The value at $\theta = 0°$ for the hexagonal bridge antenna is 5.603-dB lower than that of the standard gain antenna, translating to an absolute gain of 1.52 dBi. This value is close to the gain reported in [18].

Table 1 summarizes the measured gains of the two antennas using the image and NF comparison methods, along with the simulated gains. Both methods exhibit excellent accuracy in the estimation of antenna gain.

A 1 × 4 DUAL-POLARIZED PHASED ARRAY

The NF-to-FF method is particularly handy for characterizing the absolute gain, radiation pattern, and scan performance of mm-wave phased arrays. A good example is the measurement of a dual-band, dual-polarized phased array reported in [18]. In [18], calibrated NF data of each element are directly used to compute the absolute gain and scan patterns of the array. A detailed measurement procedure and results can be found in the published article and are therefore not repeated here. In summary, the proposed NF-to-FF technique is easy to implement and can provide excellent accuracy in characterizing the gain and radiation pattern of a probe-fed mm-wave antenna or array.

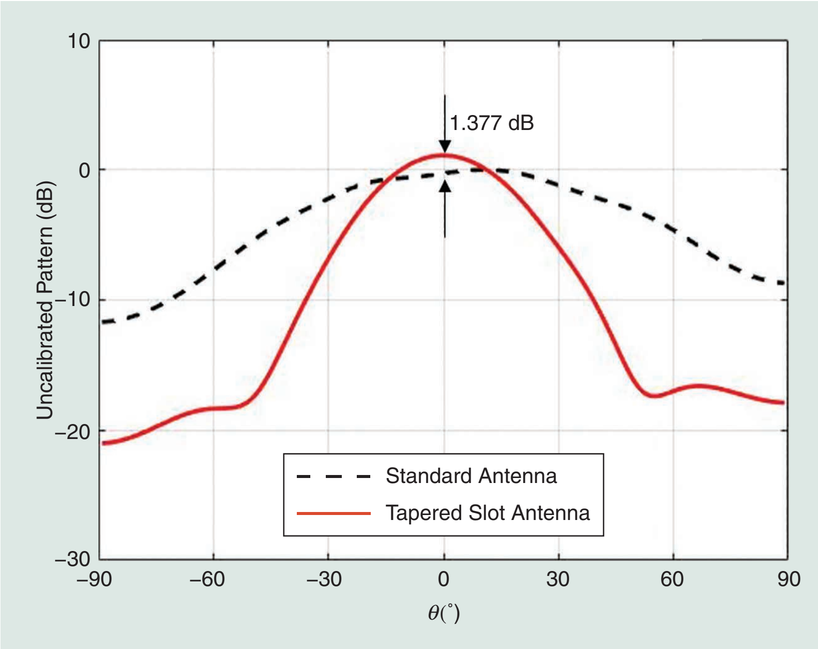

FIGURE 11. Uncalibrated radiation patterns of the tapered slot and standard gain antennas in the *xz*-plane.

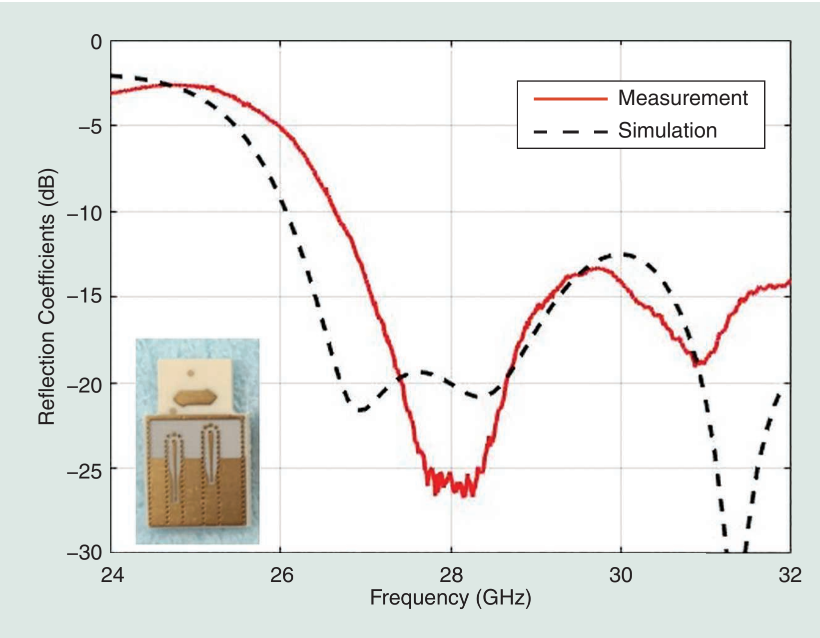

FIGURE 12. The fabricated hexagonal bridge antenna and its reflection coefficients.

TABLE 1. ABSOLUTE GAIN OF THE TAPERED SLOT AND HEXAGONAL BRIDGE ANTENNAS AT 28 GHZ.

	Simulation (dBi)	Image Method (dBi)	NF-to-FF Method (dBi)
Tapered slot antenna	8.9	8.4	8.5
Hexagonal bridge antenna	1.15	1.16	1.52

CONCLUSION

In this article, an NF-based setup was used for reflection coefficients and gain and radiation pattern measurements of probe-fed mm-wave antennas. Two gain measurement techniques were demonstrated. The image method is a simple, precise, and inexpensive way of measuring the gain of linearly polarized antennas. The NF-to-FF method can measure both the gain and radiation patterns of antennas with any polarizations. A probe-fed, ground-backed dipole antenna was designed, fabricated, and characterized using the image method. It was then used as the standard gain antenna in the NF-to-FF gain measurement to characterize the gain of a tapered slot antenna.

Unlike most FF antenna measurement setups that require expensive anechoic chambers and customized fixtures [2], [3], [4], [5], our setup consists of only basic test equipment that is commercially available. This significantly lowers the required space and costs of testing. More importantly, the method can be directly implemented on a conventional probe station in a straightforward manner. The accuracy and repeatability of antenna gain and pattern measurements were demonstrated in the article.

Although the EO NF system and image method have been presented in the literature, it is the first time that these techniques have been combined into a systematic approach and implemented on probe-fed mm-wave antennas. We believe that this technique is timely due to the proliferation of integrated mm-wave antennas for 5G and 6G mobile devices. It could facilitate probe-fed mm-wave antenna measurements and spark inspiration to further improve antenna measurement setups in the future.

ACKNOWLEDGMENT

The NeoScan system used in the measurement was commercialized by EMAG Technologies, for which Kamal Sarabandi is a principal.

AUTHOR INFORMATION

Menglou Rao (menglrao@umich.edu) is with the Radiation Laboratory, Electrical

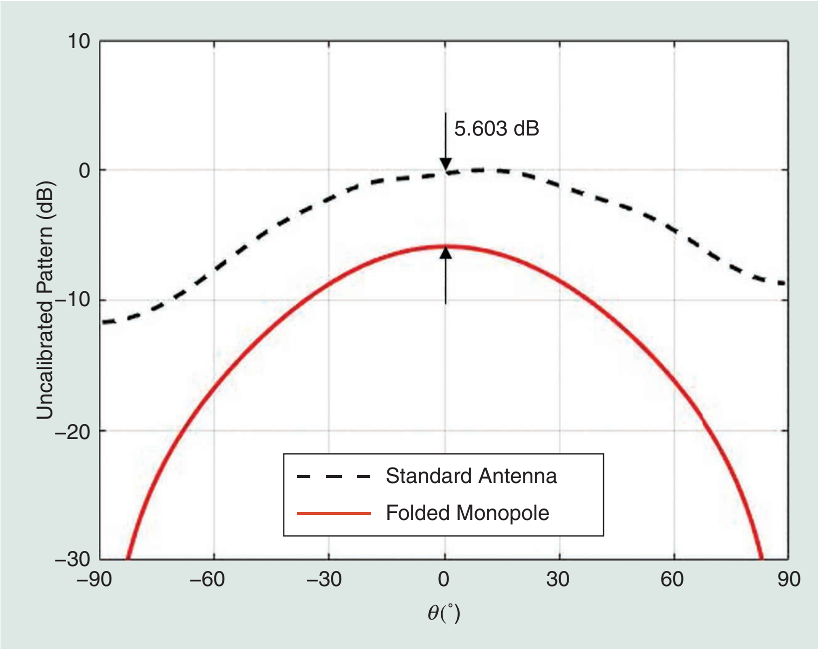

FIGURE 13. Uncalibrated radiation patterns of the hexagonal bridge and the standard gain antennas in the *xz*-plane.

Engineering and Computer Science Department, University of Michigan, Ann Arbor, MI 48109 USA. She is a Student Member of IEEE.

Kamal Sarabandi (saraband@umich.edu) is with the Radiation Laboratory, Electrical Engineering and Computer Science Department, University of Michigan, Ann Arbor, MI 48109 USA. He is a Life Fellow of IEEE.

REFERENCES

[1] S. Ranvier, M. Kyrö, C. Icheln, C. Luxey, R. Staraj, and P. Vainikainen, "Compact 3-D on-wafer radiation pattern measurement system for 60 GHz antennas," *Microw. Opt. Technol. Lett.*, vol. 51, no. 2, pp. 319–324, Feb. 2009, doi: 10.1002/mop.24034.

[2] R. N. Simons and R. Q. Lee, "On-wafer characterization of millimeter-wave antennas for wireless applications," *IEEE Trans. Microw. Theory Techn.*, vol. 47, no. 1, pp. 92–96, Jan. 1999, doi: 10.1109/22.740086.

[3] R. N. Simons, "Novel on-wafer radiation pattern measurement technique for MEMS actuator based reconfigurable patch antennas," NASA Glenn Research Center, Cleveland, OH, USA, Technical Memorandum, NASA/TM-2002-211816, Oct. 2002.

[4] N. Behdad, D. Shi, W. Hong, K. Sarabandi, and M. P. Flynn, "A 0.3 mm^2 miniaturized X-band on-chip slot antenna in 0.13 µm CMOS," in *Proc. IEEE Radio Freq. Integr. Circuits Symp.*, 2007, pp. 441–444, doi: 10.1109/RFIC.2007.380919.

[5] K. Van Caekenberghe et al., "A 2–40 GHz probe station based setup for on-wafer antenna measurements," *IEEE Trans. Antennas Propag.*, vol. 56, no. 10, pp. 3241–3247, Oct. 2008, doi: 10.1109/TAP.2008.929433.

[6] A. Shamim, L. Roy, N. Fong, and N. G. Tarr, "24 GHz on-chip antennas and balun on bulk Si for air transmission," *IEEE Trans. Antennas Propag.*, vol. 56, no. 2, pp. 303–311, Feb. 2008, doi: 10.1109/TAP.2007.915421.

[7] A. Jam and K. Sarabandi, "A submillimeter-wave near-field measurement setup for on-wafer pattern and gain characterization of antennas and arrays," *IEEE Trans. Instrum. Meas.*, vol. 66, no. 4, pp. 802–811, Apr. 2017, doi: 10.1109/TIM.2017.2654128.

[8] K. Yang, "Electrooptic mapping and finite-element modeling of the near-field pattern of a microstrip patch antenna," *IEEE Trans. Microw. Theory Techn.*, vol. 48, no. 2, pp. 288–294, Feb. 2000, doi: 10.1109/22.821779.

[9] K. Sabet, R. Darragh, A. Sabet, K. Sarabandi, and L. P. B. Katehi, "Using electro-optic field mapping for design of dual-band circularly polarized active phased arrays," in *Proc. IEEE 18th Wireless Microw. Technol. Conf. (WAMICON)*, Jan. 2017, pp. 1–5, doi: 10.1109/WAMICON.2017.8023961.

[10] K. Sabet, R. Darragh, A. Sabet, K. Sarabandi, K. Jamil, and S. Alhumaidi, "Characterization and diagnostics of active phased array modules using non-invasive electro-optic field probes with a CW laser source," in *Proc. IEEE MTT-S Int. Microw. Symp. Dig.*, 2017, pp. 1617–1619, doi: 10.1109/MWSYM.2017.8058944.

[11] K. Sarabandi, J. Choi, A. Sabet, and K. Sabet, "Pattern and gain characterization using nonintrusive very-near-field electro-optical measurements over arbitrary closed surfaces," *IEEE Trans. Antennas Propag.*, vol. 65, no. 2, pp. 489–497, Feb. 2017, doi: 10.1109/TAP.2016.2633949.

[12] G. Gaborit, P. Artillan, C. Bermond, G. Revillod, G. Chevrier-Gros, and L. Duvillaret, "20 GHz antenna radiation pattern obtained from near-field mapping with electrooptic probe on a single plane," *IEEE Antennas Wireless Propag. Lett.*, vol. 19, no. 7, pp. 1177–1181, Jul. 2020, doi: 10.1109/LAWP.2020.2994263.

[13] A. C. Newell, R. D. Ward, and E. J. McFarlane, "Gain and power parameter measurements using planar near-field techniques," *IEEE Trans. Antennas Propag.*, vol. 36, no. 6, pp. 792–803, Jun. 1988, doi: 10.1109/8.1181.

[14] "NeoScan, ultra-wideband non-invasive field measurement system." Accessed: May 25, 2022. [Online]. Available: https://emagtech.com/neoscan-system/

[15] R. Montoya Moreno, J. Ala-Laurinaho, A. Khripkov, J. Ilvonen, and V. Viikari, "Dual-polarized mm-Wave endfire antenna for mobile devices," *IEEE Trans. Antennas Propag.*, vol. 68, no. 8, pp. 5924–5934, Aug. 2020, doi: 10.1109/TAP.2020.2989556.

[16] H. Li, Y. Li, L. Chang, W. Sun, X. Qin, and H. Wang, "A wideband dual-polarized endfire antenna array with overlapped apertures and small clearance for 5G millimeter-wave applications," *IEEE Trans. Antennas Propag.*, vol. 69, no. 2, pp. 815–824, Feb. 2021, doi: 10.1109/TAP.2020.3016512.

[17] W. Sun, Y. Li, L. Chang, H. Li, X. Qin, and H. Wang, "Dual-band dual-polarized microstrip antenna array using double-layer gridded patches for 5g millimeter-wave applications," *IEEE Trans. Antennas Propag.*, vol. 69, no. 10, pp. 6489–6499, Apr. 2021, doi: 10.1109/TAP.2021.3070185.

[18] M. Rao and K. Sarabandi, "A low-profile dual-band dual-polarized quasi-endfire phased array for mmWave 5G smartphones," *IEEE Access*, vol. 10, pp. 38,523–38,533, Apr. 2022, doi: 10.1109/ACCESS.2022.3165562.

[19] S. Silver, *Microwave Antenna Theory and Design*. New York, NY, USA: McGraw-Hill, 1949.

[20] P. Coquet, K. Mahdjoubi, and C. Terret, "Automatic antenna gain measurement at high frequencies," *Electron. Lett.*, vol. 28, no. 14, pp. 1339–1340, Jul. 1992, doi: 10.1049/el:19920850.

[21] G. Felic, "Antenna gain measurements in the V-band: A single-antenna method," in *Proc. 2009 Electromagn. Compat. Symp. Adelaide (EMCSA)*, pp. 98–101.

[22] J. Zheng, J. Ala-Laurinaho, and A. V. Raisanen, "On the one-antenna gain measurement method in probe station environment at mm-Wave frequencies," *IEEE Trans. Instrum. Meas.*, vol. 68, no. 11, pp. 4510–4517, Nov. 2019, doi: 10.1109/TIM.2018.2890454.

[23] C. A. Balanis, *Antenna Theory: Analysis and Design*, 3rd ed. Hoboken, NJ, USA: Wiley, 2005.

[24] S. Beer and T. Zwick, "Probe based radiation pattern measurements for highly integrated millimeter-wave antennas," in *Proc. 2010 4th Eur. Conf. Antennas Propag. (EuCAP)*, pp. 1–5.

[25] A. Shamim, L. Roy, N. Fong, G. Tarr, and V. Levenets, "On-chip antenna measurements: Calibration and de-embedding considerations," in *Proc. IEEE Instrum. Meas. Technol. Conf.*, 2005, vol. 1, pp. 463–466, doi: 10.1109/IMTC.2005.1604158.

[26] J. Ala-Laurinaho, J. Zheng, and A. V. Raisanen, "One-antenna gain measurement in a probe station," in *Proc. 2018 IEEE Conf. Antenna Meas. Appl. (CAMA)*, pp. 28–31.

[27] H. Kim and C. W. Jung, "Ultra-wideband endfire directional tapered slot antenna using CPW to wide-slot transition," *Electron. Lett.*, vol. 46, no. 17, pp. 1183–1185, Sep. 2010, doi: 10.1049/el.2010.1792.

[28] R. E. Collin, *Antennas and Radiowave Propagation*. New York, NY, USA: McGraw-Hill, 1985.